Thin Polymer Brush Decouples Biomaterial's Micro-/Nano-Topology and Stem Cell Adhesion

Michel Klein Gunnewiek, Edmondo M. Benetti, Andrea Di Luca, Clemens A. van Blitterswijk, Lorenzo Moroni, and G. Julius Vancso**

M. Klein Gunnewiek, Prof. G.J. Vancso, Department of Materials Science and Technology of Polymers, University of Twente, MESA+ Institute for Nanotechnology, P.O. Box 217, 7500 AE Enschede, The Netherlands. Fax: 0031 53 489 3823; Tel: 0031 53 489 2974; E-mail: g.j.vancso@utwente.nl

Dr. E.M. Benetti, Laboratory for Surface Science and Technology, Department of Materials, ETH Zurich, Wolfgang-Pauli-Strasse 10, 8093 Zurich, Switzerland.

Andrea Di Luca, Dr. L. Moroni, Department of Tissue Regeneration, MIRA Institute for Biomedical Technology and Technical Medicine, University of Twente, P.O. Box 217, 7500 AE Enschede, The Netherlands, Fax: 0031 53 489 2150; Tel: 0031 53 489 3400; E-mail: l.moroni@utwente.nl

Keywords: cell morphology; mesenchymal stem cells; poly(ε-caprolactone); polymer brushes; surface topology

Surface morphology and chemistry of polymers used as biomaterials, such as tissue engineering scaffolds, have a strong influence on the adhesion and behavior of human mesenchymal stem cells. Here we studied semicrystalline poly(ε-caprolactone) (PCL) substrate scaffolds, which exhibited a variation of surface morphologies and roughness originating from different spherulitic superstructures. Substrates were obtained by varying the parameters of the thermal processing, i.e. crystallization conditions. The cells attached to these polymer substrates adopted different morphologies responding to variations in spherulite density and size. In order to decouple substrate topology effects on the cells, sub-100 nm bio-adhesive polymer brush coatings of oligo(ethylene glycol) methacrylates were grafted from PCL and functionalized with fibronectin. On surfaces featuring different surface textures, dense and sub-100 nm thick brush coatings determined the response of cells, irrespective to the underlying topology. Thus, polymer brushes decouple substrate micro-/Nanoscale surface topology and the adhesion of stem cells.

Introduction

Cell-biomaterial interactions have been increasingly studied in the last decade aiming to shed light on the mechanisms which govern cellular attachment and proliferation. Thus, increasing efforts have been dedicated to replicate the characteristics of natural tissues by engineering synthetic extra-cellular matrix (ECM) environments. Hereby particular attention has been paid to structural details, bulk physical properties and cytocompatibility of the synthetic substrates. Morphological and chemical structuring of surfaces have been demonstrated to influence the behavior of adhering cells, with differences depending on cell type. Similar ECM manipulations have been demonstrated to trigger a cascade of biomolecular events which eventually contribute to determining cells' fate.[1-2] In this respect, particular interest was devoted to stem cells, and

specifically to human mesenchymal stem cells (hMSCs), as starting platforms for possible new tissue regeneration strategies.[3-4] These are adult cells of easy accessibility, which possess the capability to differentiate in various lineages such as neuronal[5], myotic[6] or osteoblast-like cells[7]. Different environmental parameters were recently demonstrated to control hMSCs activity, and thus stability, morphology, proliferation and differentiation. Among these, ECM elasticity,[8] micro-/nano-topology,[9-10] and availability of ligands[11] represented the main determining factors. As a general approach, all the fabrication methods aiming at directing particular stem cells' lineage specification have been centered on mimicking the corresponding natural tissue environments.[2, 12] Additionally, a direct consequence of hMSCs behavior was related to artificial ECM-driven changes in cell shape.

In particular, different biomaterials' surface roughness[13-14] and micro/nano-patterned topology[15-17] have been demonstrated to determine hMSCs adhesion and behavior. Namely, cells incubated on different patterned substrates could preferentially differentiate into neuronal, osteogenic or adipogenic lineages[18-19]. In these experiments, controlled structuring of the topology at the scaffold interface translated into a morphological response by the adhered cells, which subsequently lead to a preferential differentiation towards a defined cell tissue type.

Increasing attention has, thus, been devoted to the physico-chemical properties of cell-biomaterial interfaces, which determine the performance of the matrix i.e. cells-biomaterial adhesion and scaffold integration in the natural tissue environment. Among the engineering methods used to tune all the characteristics relevant for biomaterial surfaces, polymer grafting represents one of the most attracting and promising strategies. Densely surface-grafted polymers, also termed brushes, proved to be versatile coatings featuring tailorable chemistries, multifunctionalities and responsive behavior.[20-21] Their application as coatings allow one to tune

interfacial properties, which are highly relevant for biological systems, such as swelling (directly determining bio-adhesion),[22-24] stiffness, and controlled exposure of biological cues.[25-26] Specifically, adhesive biomolecules such as arginine-glycine-aspartic acid sequences (RGD), fibronectin (FN), or collagen have been immobilized on brush films obtaining multilayered architectures which strongly enhanced the cell-substrate affinity.[27-28]

Polymer brushes have been broadly applied as surface modifiers for biomaterials. Specifically the multi-functional and morphological characteristics of densely grafted films have been exploited to design bio-passive and bio-functional films regulating the interaction between biomaterials and cells, proteins or bacteria.[20-21] In particular the highly hydrated nature of poly(ethylene glycol) (PEGs)-based brushes (or analogues)[29-31] provided biopassivity to organic and inorganic surfaces.[32-34] On the contrary, high density of functions on bio-adhesive brushes allowed an enhanced surface-loading of ECM proteins during cell culturing thus triggering biological adhesion.[26-27, 33]

In this work, we particularly focus on the decoupling effect by cell-adhesive brushes between different surface topologies and hMSCs adhesion. To this aim, we employed surface-initiated atom transfer radical polymerization (SI-ATRP)[21, 35] of oligo(ethylene glycol) (OEG) methacrylates[34, 36-37] to generate functionalizable sub-100 nm brush layers which, following FN immobilization, were finally applied as study platforms for the adhesion of hMSCs.

Poly(ε-caprolactone) (PCL) films were used as substrates for brush growth. This thermoplastic biodegradable polymer has been extensively used for the fabrication of scaffolds as supports for cells culturing, due to its excellent biocompatibility.[38-40] In particular, PCL is attractive due to its long term degradation, good solubility in different solvents and high permeability to drugs.[41] In order to produce different surface topologies on PCL surfaces, spin-coated films were subjected

to different thermal treatments from melts, resulting in alternatively fast and slow crystallization. Thus, tuning of the assembly kinetics of polymer chains into lamellar structures determined the density and size of PCL spherulites, which in-turn influenced the substrate micro-/nano-topologies. This method represented an effective and costless strategy to introduce different topologies with diverse orders of periodicities and pattern types (Scheme 1a-c).

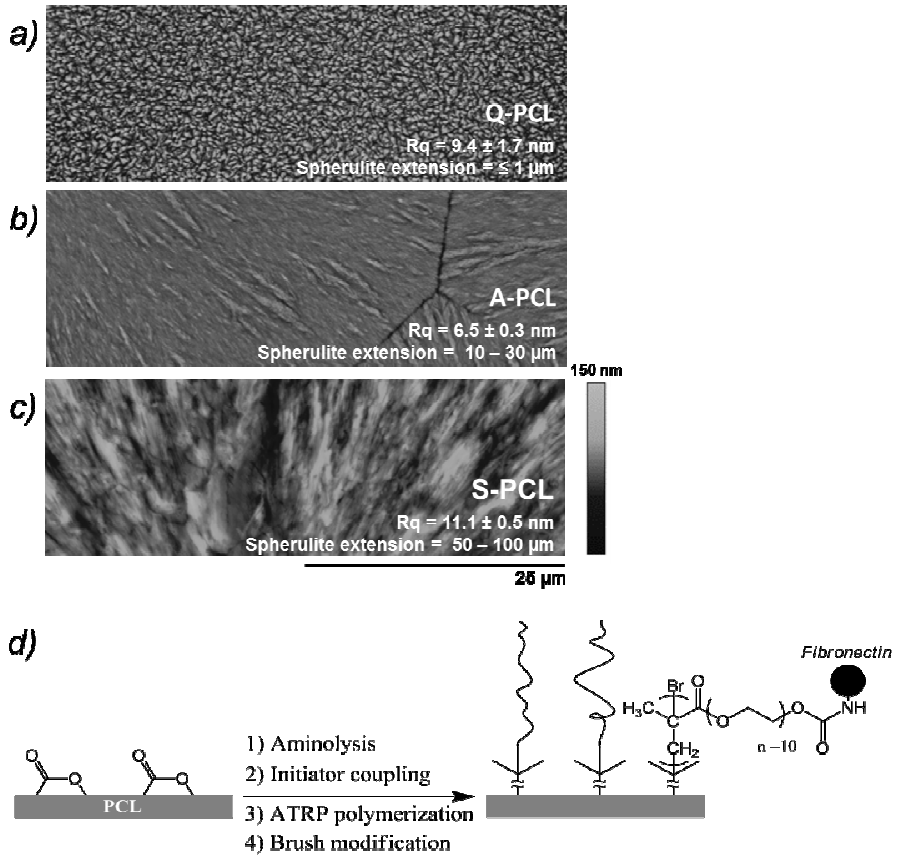

Scheme 1: Preparation of PCL surfaces by different thermal processing to obtain Q-PCL (a), A-PCL (b) and S-PCL (c). Subsequent POEGMA grafting by SI-ATRP on the different PCL topologies and FN coupling on tethered polymer's side chains (d).

These different PCL films were treated with FN and subsequently incubated with hMSCs to investigate the effect of different topologic parameters on cell adhesion. Alternatively, they were

used as precursor surfaces for the fabrication of sub-100 nm POEGMA cell-adhesive brushes. The interfacial effect of uniform brush coatings on different semicrystalline topologies was finally studied by assessing the morphological response of adhered hMSCs. An in-depth focus was furthermore given to the capability of POEGMA brushes to efficiently tune cell adhesion irrespective to the underlying substrate characteristics (roughness and surface morphology). Brush coatings for scaffolds and tissue engineering supports would additionally confer function and tunable surface properties to these biomaterials.

Materials and Methods

Materials: Oligo(ethylene glycol) methacrylate (OEGMA, Aldrich, Mn = 526 g/mol) was purified from hydrochinone inhibitors by passing it through a basic alumina column using dichloromethane (DCM, Biosolve) as an eluent. Afterwards DCM was removed under vacuum. Copper(I) chloride (CuCl, Aldrich, 98%) was purified by stirring in glacial acetic acid, filtering, and washing with ethanol three times, followed by drying in vacuum at room temperature overnight. Copper(II) bromide (Sigma-Aldrich, ≥99%), methanol (Biosolve, absolute), isopropanol (iPA, Biosolve), ethylenediamine (EDA, Sigma-Aldrich, ≥99%), dry hexane (Acros, Extra Dry over Molecular Sieve, 97%), N,N-Dimethylformamide (DMF) (Acros, Extra Dry over Molecular Sieve, 99,8%), pyridine (Sigma-Aldrich, anhydrous, 99,8%), 2,2'-bipyridil (BiPy) (Sigma-Aldrich, ≥99%), 2-bromoisobutyryl bromide (BIBB) (Aldrich, 98%), Ethylenediaminetetraacetic acid disodium salt dihydrate (EDTA) (Sigma, 99%), 4-dimethylaminopyridine (DMAP) (Sigma-Aldrich, ≥99%), N,N´-disuccinimidyl carbonate (Sigma-Aldrich, 98%), triethylamine (Sigma-Aldrich, ≥99%), and FN (Invitrogen) were used as received. All water used in the experiments was Millipore Milli-Q grade. Basic cell culture media was prepared by adding to a α-MEM cell medium (Invitrogen), 10 v/v% of Fetal Bovine

Serum (FBS), 2 mM of L-Glutamine, 100 U/mL of penicillin, 100 µg/mL of streptomycine, and 0.2 mM of ascorbic acid. All the mentioned components were obtained from Invitrogen. Furthermore, Invitrogen provided phosphate buffered saline (PBS), bovine serum albumin (BSA), trypsin, 4',6-diamidino-2-phenylindole (DAPI), fluorescein isothiocyanate (FITC). Formalin (neutral buffered, 10%) and triton x-100 were both purchased from Sigma-Aldrich.

Activation of the polymer films: Silicon or glass substrates were first cleaned with Piranha solution, then rinsed extensively with water and ethanol. Caution: Piranha solution reacts violently with many organic materials and should be handled with great care! PCL films were spin coated (2000 rpm for 1 minute) onto the cleaned substrates from a chloroform solution (1 wt%). Subsequently, the PCL films were annealed at 70 °C for 1 hour and cooled down by either quenching the films in liquid nitrogen (Q-PCL), removing the films from the oven and cooling to ambient temperature (A-PCL), or by slow cooling at 0.5 °C/min (S-PCL). The differently treated PCL films were subsequently immersed into a solution of 5 mM ethylenediamine (EDA) in isopropanol (iPA). The reaction was allowed to proceed for 10 minutes under room temperature conditions. Samples were then rinsed with ice-cold water and subsequently rinsed with water at room temperature, then dried in a stream of nitrogen. (2) The aminated PCL films were immersed into 10 ml of dry hexane and 100 µL of dry pyridine, to which 100 µL of 2-bromoisobutyryl bromide (BIBB) was added dropwise. The reaction mixture was gently stirred for 1 hours at room temperature to produce the 2-bromoisobutyryl-immobilized PCL surface (the PCL-Br surface). The PCL-Br substrate was then washed repeatedly with a methanol/water (1/1, v/v) mixture and dried under a stream of nitrogen.

Atom transfer radical polymerization (ATRP) of OEGMA brushes: Purified OEGMA monomer (5 g, 9.5 mmol) and 2,2'bipyridine (81.7 mg, 0.52 mmol) were added to a water (5ml) and

methanol (1,26ml) mixture. The solution was purged with nitrogen for 30 min. CuCl (18.75 mg, 0.19 mmol) and $CuBr_2$ (2 mg, 0.009 mmol) were added into another reaction flask and also flushed with nitrogen. Monomer, ligand and catalyst were then combined and stirred for another 30 minutes to facilitate the formation of the organometallic complex. This solution was then transferred into the flasks containing the activated PCL substrates. The flasks were sealed with rubber septa and kept at room temperature under nitrogen. After reaching the desired reaction time of 60 minutes, the substrates were removed from the polymerization solution, exhaustively rinsed with water to remove any unreacted and not surface tethered substances and subsequently dried in a stream of nitrogen. Afterwards the samples were washed with a 0.1M EDTA solution overnight to extract the copper from the polymer brushes.

Fibronectin functionalization: The samples were placed in a dry DMF solution containing 100 mM of DSC, DMAP and TEA. Subsequently the samples were incubated in a 0,1 mM FN solution overnight in order to covalently couple the FN to the polymer brush. On the contrary, pure PCL substrates were incubated in a 0,01 mM FN solution overnight to ensure a final surface concentration of FN comparable to the brush-coated corresponding samples (SI for supporting XPS data)

Cell culture and cell image analysis: Human mesenchymal stem cells were cultured at 37°C in a humidified atmosphere of 5% carbon dioxide, using as culture medium α-MEM supplemented with 10 v/v % FBS, 2 mM L-Glutamine, 1 mM sodium pyruvate, 100 U/mL of penicillin and 100 μg/mL of streptomycin. The cells were seeded at a density of 2,000 cells/cm^2 on PCL substrates, unmodified and modified with POEGMA brushes. After 4 hours, the substrates were washed twice with PBS and fixed with a 3.7 v/v % formaldehyde solution in PBS for 10 minutes at room temperature. Next, the samples were washed two or more times with PBS containing 1

w/v % bovine serum albumin (BSA). Cell membrane was permeabilized by treating the samples with 0.1 v/v % Triton X-100 solution in PBS-BSA after which the specimens were washed again with PBS-BSA. Cell nuclei were stained with DAPI diluted 1:100 and cell cytoskeleton was stained with a phalloidin-rhodamine FITC solution diluted 1:50 in a PBS-BSA for 30 minutes at room temperature. Pictures were taken using a Nikon fluorescent microscope Eclipse E600. In order to use the samples for optical and AFM imaging, the substrates were dehydrated by submerging the samples into a solution for 10 minutes containing an increasing amount of ethanol. Optical imaging was performed on a BX60 optical microscope (Olympus, Tokyo, Japan). For determining the cell shape parameters area and perimeter, Cell^D software (Olympus Soft Imaging Solutions, Münster, Germany) was used. The Roundness (RN) was subsequently calculated using: $RN=Perimeter/(4\pi \times Area)^{0.5}$.[42] To test the statistical significance of the difference in the cell shape parameters, a one-way ANOVA test followed by a Tukey's post-hoc test was performed. Statistical significance was set at a p value of 0.05.

AFM Imaging: A Dimension D3100 AFM equipped with a hybrid scanner and a NanoScope IVa controller (Digital Instruments, Veeco-Bruker, Santa Barbara, CA) was operated in tapping mode using commercially available silicon cantilevers (PointProbe® Plus silicon probes, PPP-NCH, Nanosensors, Neuchatel, Switzerland) to obtain the surface morphology of the PCL substrates.

Results and Discussion

Three different semi-crystalline topologies were obtained on 100 nm thick spin-coated PCL films by first annealing the films at 75°C and subsequently applying different cooling rates, namely (i) quenching of crystallization by dipping the samples in liquid N_2, (ii) fast cooling at room temperature and (iii) slow cooling at 0.5 °C/min. These different thermal treatments determined PCL crystallization and, consequently, the topology of the exposed interfaces, as can be seen in

the atomic force microscopy (AFM) micrographs reported in Schemes 1a-c. Quenched PCL films showed sub-micron sized spherulitic structures (up to 1 μm) (Scheme 1a, samples labelled as Q-PCL) uniformly and densely covering the whole film. On the contrary, slower cooling rates triggered the formation of larger spherulites ranging from sub-50 μm (Scheme 1b, samples labeled as A-PCL) to several hundred μm (Scheme 1c, samples labeled as S-PCL). In the two last cases, lamellar aggregates expand from the center of nucleation to the edges of the spherulites. This coarsens film topology with radial aggregates displaying typical thickness of 50-100 nm and depth of 5-10 nm (Scheme 1c). A-PCL topologies presented denser coverages of sub-50 μm, thus smaller features compared to typical hMSCs projected areas (Figure 1), while S-PCL samples displayed much larger spherulites presenting uniform lamellar expansions. These spanned over several hundreds of μm and, thus, function as homogeneously patterned areas for several adhering cells. All the so-formed PCL films were subsequently functionalized by FN through physical adsorption of the protein (functionalization steps reported in Scheme 1d and described in SI) in order to favor the adhesion of hMSCs. It is noteworthy to mention that all the obtained topologies showed similar values of roughness (Rq= 11.1±0.5, 6.5±0.3 and 9.4±1.7 nm for Q-, A- and S-PCL, respectively) as measured with AFM (sampling areas = 20 x 20 μm^2, n = 12). In addition, in all the series of different PCL samples the surface concentration of FN was kept constant as measured by XPS (XPS survey scans and data interpretation were reported in SI). Namely, ~4 * 10^{-5} and ~8 * 10^{-5} nmol/cm^2 for the pure PCL and the PCL with POEGMA brush samples.

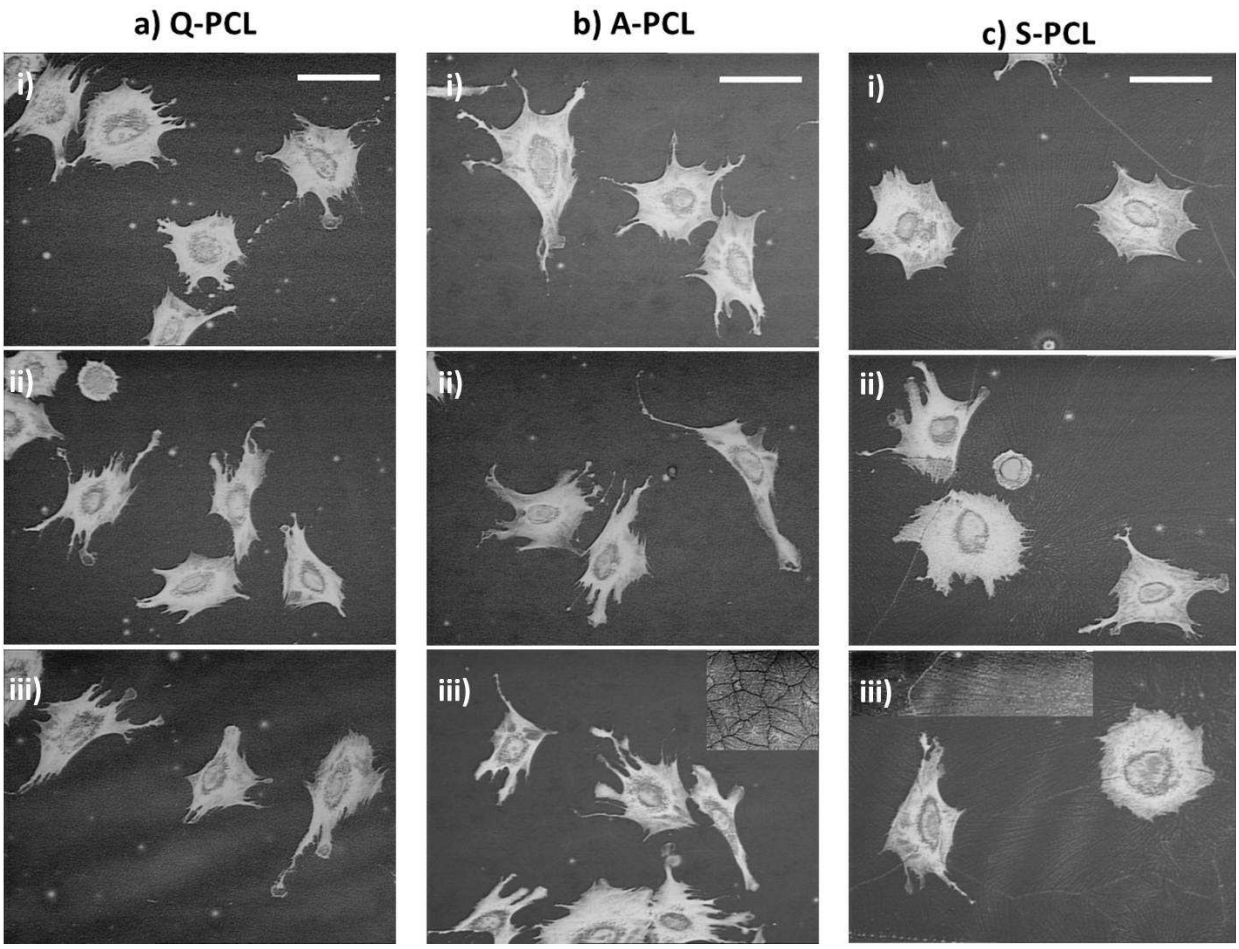

Figure 1: HMSC's adhering on Q-PCL (a), A-PCL (b) and S-PCL structures (c). Three representative images are reported for each set of samples (i, ii and iii). The insets in iii (b) and iii (c) are highly contrasted OM areas on the corresponding samples and highlight the PCL topologies at the surface. The scale bars for all the OM micrographs are 50 μm.

The morphology of hMSCs following 4 hours of incubation on the different PCL topologies was evaluated by optical (OM) and immunofluorescent microscopies concentrating on the effect of film micro-/nano-structure i.e. spherulites organization and size. Generally, hMSCs morphology responded to differences in semicrystalline topologies of PCL. This can be seen in Figures 1 and 2. hMSCs adhering on sub-micron Q-PCL and small spherulites typical of A-PCL showed

branching and irregular shapes (Figure 1a and b), also confirmed by immunofluorescence imaging (Figure 2).

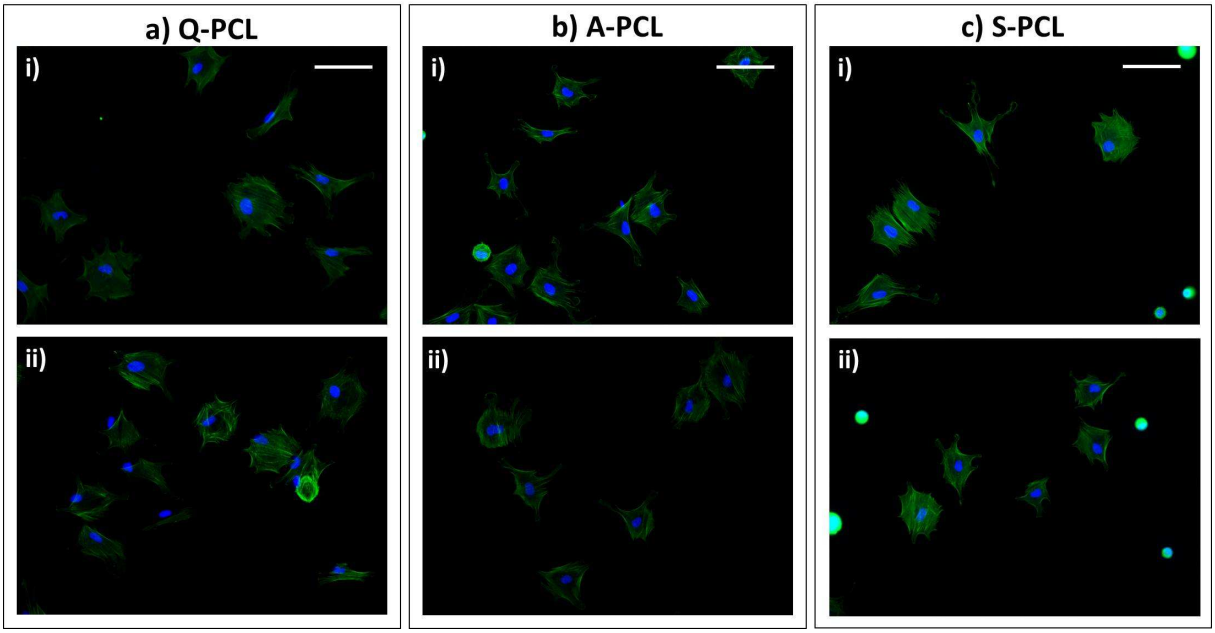

Figure 2: Immunofluorescence images of hMSCs adhered on a) Q-PCL, b) A-PCL and c) S-PCL topologies following 4 hours of incubation. The scale bars for all the fluorescent images are 100 μm.

On the contrary hMSCs incubated on large spherulitic organizations (S-PCL) displayed more regular and symmetric shapes with limited branching (Figures 1c and 2c). Evaluation of cell parameters calculated from OM and immunofluorescence images corroborated the qualitative analysis of hMSCs morphology upon adhesion on the different PCL topologies. In Figure 3 average values of cells area, perimeter (P) and roundness (RN) are reported for all the PCL samples studied. hMSCs projected areas increased with the size of the spherulitic patterns ($P<0.05$ between Q-/A-PCL and S-PCL). Simultaneously, both P and RN decremented for cells adhering on S-PCL compared to Q- and A-PCL samples ($P<0.05$).

In summary, dense assemblies of sub-50 µm spherulites (shown in Q- and A-PCL) induced cells to adapt to irregular and disperse features presenting lamellar aggregates which expand in all directions and across variable surface radii. On these samples hMSCs' projection covered several spherulites and cells were thus shown to respond to these disconnected features by an irregular spreading and a more pronounced branching.

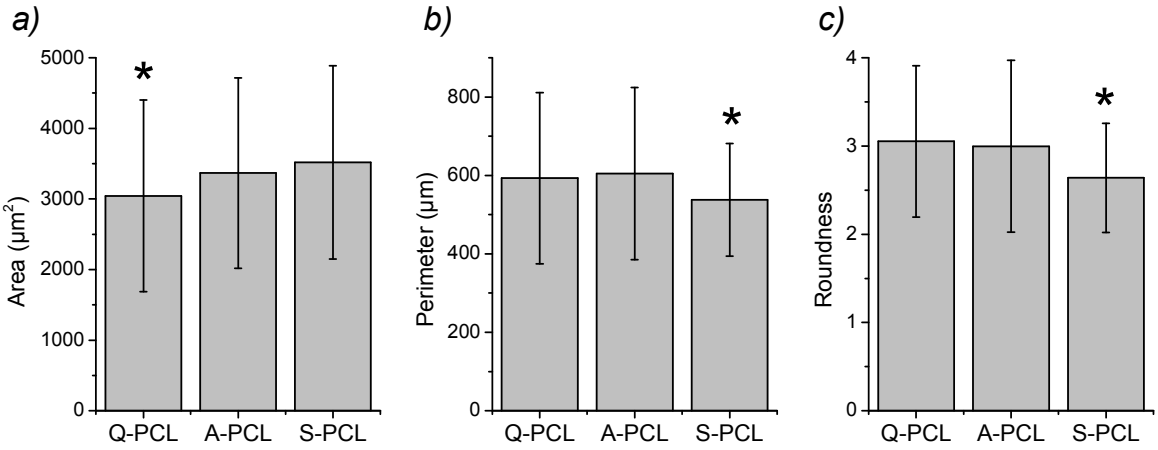

Figure 3: Projected area a), perimeter b) and roundness values c) of cell adhering on PCL with different topologies (Q-PCL, A-PCL and S-PCL). * denotes statistical significant differences between the assigned and the non-assigned topologies ($p < 0.05$).

Conversely, when incubated on extended lamellar patterns developing over hundreds of µm, cells adopted more symmetrical and regular shapes with larger projected areas (Figure 1 and 2). In these cases the increase of symmetry and regularity by cells' morphology were also recorded as a decrease in the average values of P and RN (Figure 3).

The roles played by surface roughness and pattern type on the adhesion and the behavior of hMSCs have been studied during the last decade.[5, 43-45] Namely, different patterns induced

specific cell orientation and stretching by contact guidance, which in some cases also affected their differentiation.[5, 43] In addition, different roughness on inorganic and polymeric supports was shown to affect the density of adhering hMSCs.[46-47] In this context, the simple processing method proposed here represents an effective and low-cost strategy to introduce different topologieswith diverse orders of periodicities and different resolutions (from nano- to micro-scale) on semicrystalline supports (Scheme 1a-c). A simple control over the thermal processing conditions, often eluded during biomaterial preparations, turned into tuning over surface features and hMSCs adhesion.

Having established the dependence of hMSCs morphology on substrate features (type and extension), we subsequently investigated the activity by a thin brush coating on cell-topology interactions. In order to accomplish this, the different PCL supports were coated with a sub-100 nm POEGMA brush by PCL chemical activation, following SI-ATRP.[24, 27]

All POEGMA brushes grafted from PCL samples present thickness values included between 60 and 70 nm, a constant swelling ratio of around 1.1 and an average grafting density of 0.35 chains/nm^2 (measured by ellipsometry in air and aqueous environments, as reported in the experimental section and in SI). The brush coating formed thus uniformly, covering all the different PCL topological features as shown in Figure S8. POEGMA-brushes were later on "bio-activated" with FN. In POEGMA-coated PCL surfaces the protein concentration was found to be around 40 ng/cm^2 if compared to the "pure" PCL surfaces (20 ± 5 ng/cm^2 for all the different PCL topologies studied). This was due to multiple binding by POEGMA side-chains along the brush structure.[25] After 4h seeding, hMSCs morphology on brush-coated PCL topologies (named as Q-PCL-, A-PCL- and S-PCL-brush in the case of coated Q-PCL, A-PCL and S-PCL

topologies, respectively) was investigated by both OM and immunofluorescence imaging (Figure 4 and 5).

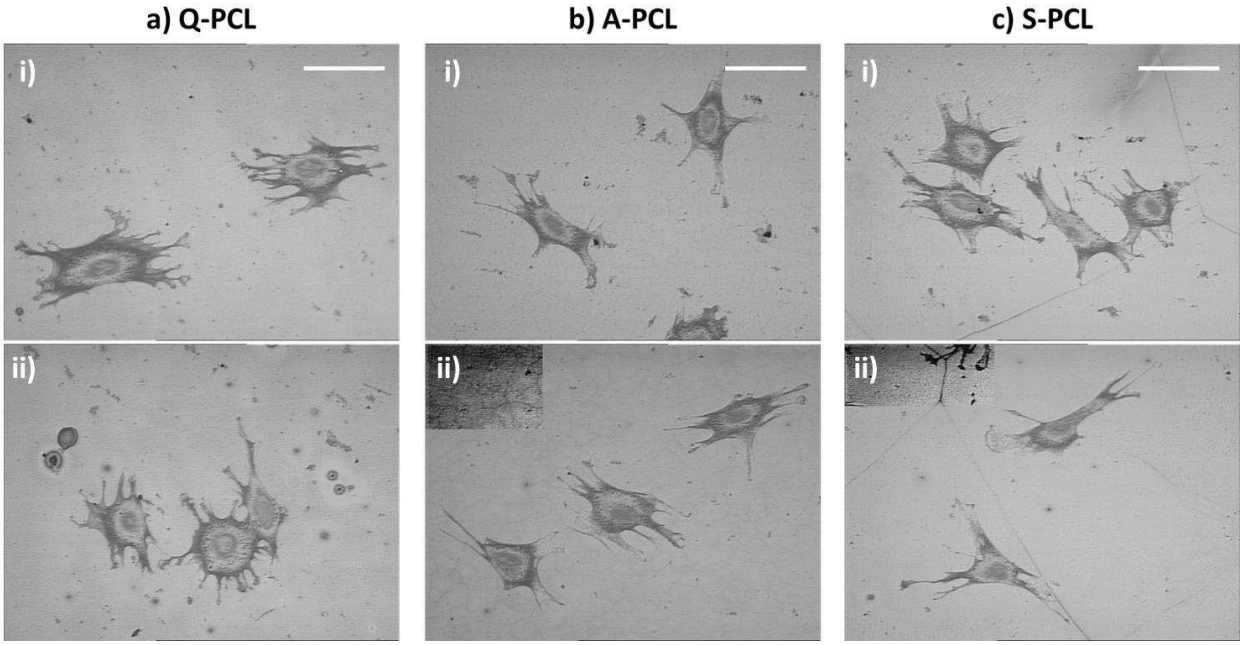

Figure 4: Optical images of cells adhering on Q-PCL (a), A-PCL (b) and S-PCL (c) with the supporting POEGMA brush. The insets in ii(b) and ii(c) are highly contrasted OM areas on the corresponding samples and highlight the brush-coated PCL topologies at the surface. The scale bars for all the OM micrographs are 50 μm.

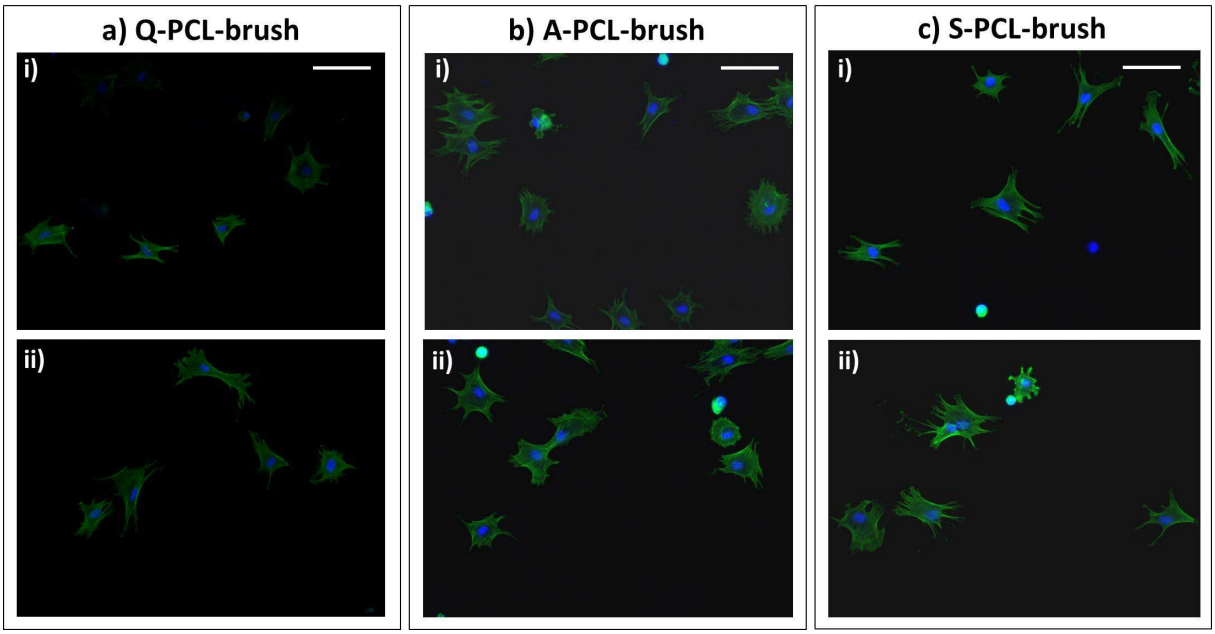

Figure 5: Immunofluorescence images of hMSCs adhered on a) Q-PCL-, b) A-PCL- and c) S-PCL-brush films following 4 hours of incubation. The scale bars for all the fluorescent pictures are 100 μm.

The same cell shape parameters were subsequently calculated from these micrographs and compared to cells adhered on the corresponding uncoated PCL samples (Figure 6).

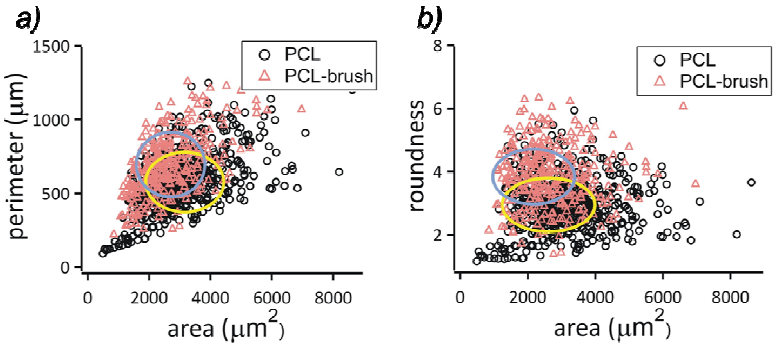

Figure 6: Perimeter a) and roundness b) plotted versus the projected area of each individual cell adhering either on a pure PCL (**O**) or on the PCL-POEGMA system (Δ).

As shown in Figure 4 and 5, hMSCs cultured on all PCL-brush surfaces showed very similar morphologies despite the underlying PCL topology. Specifically, cells were characterized by a stellate shape, a higher degree of branching and smaller projected areas if compared to cells adhered on the starting PCL samples.

Despite the higher surface concentration of FN found on the POEGMA brush, the average number of adhered cells did not increase substantially compared to uncoated PCL morphologies. Thus, given the sampling depth of XPS (around 10 nm, performed on dry POEGMA brush), we believe that the higher concentration of FN refers also to proteins within the swollen brush that are not accessible to cells. The surface density of cell-ligands was found to determine cell adhesion and spreading.[48-49] In addition, we recently reported that cell adhesion on ligand-functionalized brushes was dominated by the composition of the outer polymer brush interface.[25] Hence, assuming a comparable interfacial FN concentration between PCL and POEGMA-coated PCL, proteins exposition at the interface[50-51] together with the different physico-chemical properties of the substrates are determining factors for the different hMSCs adhesion.

In order to shed light on cell spreading mechanism onto PCL-brush in comparison to PCL uncoated films, we plotted P and RN versus projected area for each individual cell.[52] In Figure 6, the distributions of P and RN values (Figure 6a and b, respectively) for all the cells analyzed on bare PCL (black circle markers) and on the corresponding PCL-brush films (pink triangle markers) are reported. These were highlighted as colored ellipses centered on the average values and presenting semi-axes equal to the calculated standard deviations of each parameter. Thus, the difference in cell behavior between the two series of substrates could be also visualized as a degree of overlying ellipses on each graph.

The behavior of adhered hMSCs was markedly influenced by the physico-chemical nature of the polymeric supports used. The dispersion of data points reported in Figure 6a for cells attaching on brush-coated surfaces concentrated at higher P values with increasing areas, if compared to bare PCL samples. A similar trend was observed in the case of RN values in Figure 6b, where cell behavior upon spreading (towards larger areas) was characterized by RN concentrated at higher values when the substrates presented POEGMA brushes at interfaces. Thus, on PCL-brush surfaces cells generally protruded by branching and spread independently from the underlying PCL topology. On the contrary, on bare PCL hMSCs responded to the different semicrystalline features alternatively branching on small and diffused aggregates or covering larger areas and uniformly spreading on extended spherulitic organizations. The behavior of hMSCs on these surfaces was thus found substrate topology-dependent. The presence of a very thin, sub-100 nm POEGMA brush establishes the physical and chemical characteristics of the PCL interface. The interplay of amplified water content,[22-24] control exposure of protein cues,[26, 48] and film compliance,[8, 53-54] peculiar to a dense and uniform brush coating, dominates the biological response at the brush-medium interface. Hence, for all the PCL-brush samples the behavior of hMSCs was demonstrated as substrate topology-independent. From this result, we can deduce that even a very thin polymer brush significantly influences cell behavior irrespective of the underlying support characteristics in such a way that it decouples substrate nano-/micro-topology and cell response. This is particularly interesting for stem cells, as the brush-modified substrates can be proposed as a universal system to culture cells in a standardized manner without influencing their differentiation state.

The influence of a polymer brush architecture on cell adhesion has been recently investigated by us and others.[25-26] In these reports, protein ligands exposure and anchoring by densely grafted

polymer spacers were found to affect the adhesion and morphology of different cell types. In this context, the present study clarifies the fundamental activity of biomaterial-tethered brushes, which interpose flexible attachment sites for cells capable of re-organize in response to cell adhesion.[25]

POEGMA brush decoupling effect was further clarified by analyzing the behavior of hMSCs on each PCL topology before and after brush coating (Figure 7). Also in this case, we concentrated on the dispersions of P and RN values recorded for each cell adhering on the three different types of PCL surfaces as a function of the corresponding cell projected area. As it can be noticed moving from Figure 7a to 7c, i.e. following the increase of spherulite extension from Q- to S-PCL, both P and RN distributions increasingly dissociated between uncoated and coated PCL films. Hence, POEGMA brush decoupling activity was demonstrated to become more pronounced with increasing pattern extension. In conclusion, on platforms presenting topologies ranging from sub-micron aggregates to several hundred μm-extended lamellar organizations, the morphology of hMSCs was "normalized" by a dense and thin brush coating. This representation of polymer brush activity justifies their application and function as biomaterial surface-modifiers. Dense assemblies of bio-activated brushes applied to synthetic ECMs are capable of tuning the performance of the matrix by their peculiar physical properties. The exquisite combination of swelling, compliance and flexibility by tethered chains determines their function, i.e. the exposure and reception of cell cues and decoupling of substrate morphology towards cell adhesion. Particularly in the cases where contact guidance[5-7, 55-57] and roughness effects[58-60] are driving the behavior of adhering cells, brush adlayers are capable of tuning the properties of biomaterial surfaces.

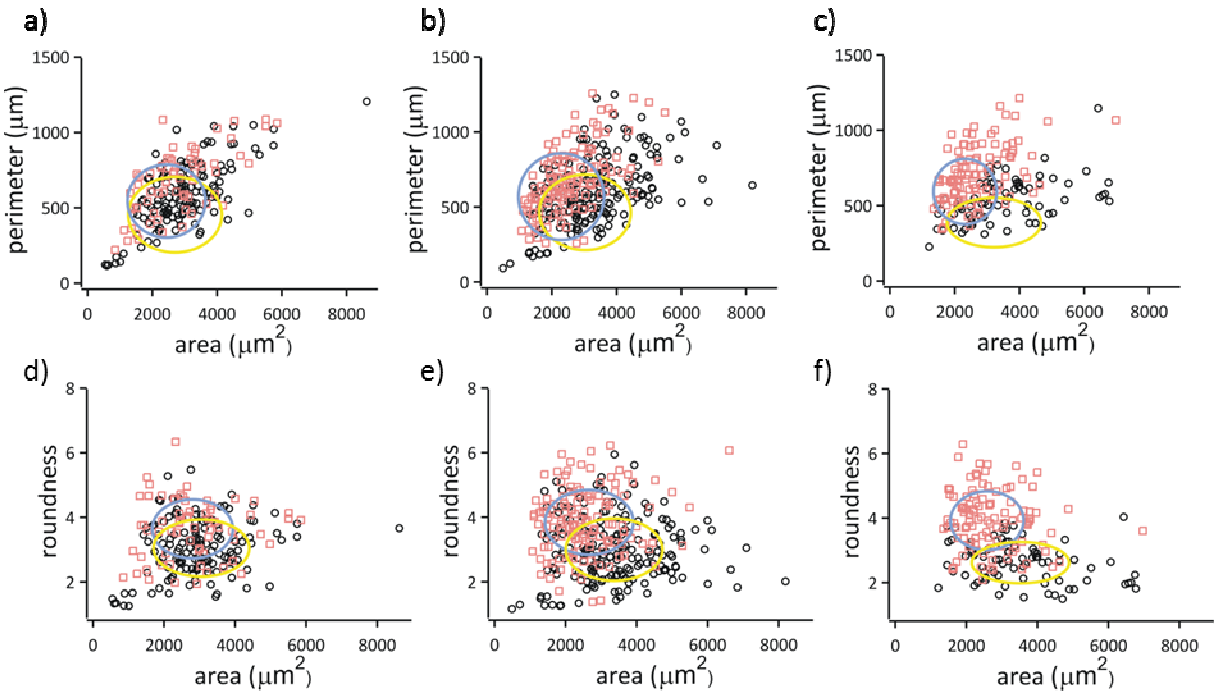

Figure 7: Perimeter (a,b,c) and roundness (d,e,f) plotted versus the projected area of each individual cell adhering either on a pure PCL (o) or on the PCL-POEGMA system (□). Q-PCL a,d), A-PCL b,e) and S-PCL c,f).

Conclusions

We describe the effects on adult bone marrow-derived mesenchymal stem cell adhesion by semicrystalline topologies of PCL supports and thin polymer brush films grafted on such substrates. Micro-/nano-topologies induced by simple thermal processing are shown to alter the behavior of hMSCs upon attachment and spreading. Cells adopt different morphologies responding to spherulite density and size. Following the coarsening and the extension of the lamellar organizations hMSCs spread more uniformly, covering increasing areas. On the contrary on sub-µm and densely dispersed semicrystalline features cells branch and adopt more irregular shapes. On these differently patterned surfaces dense and sub-100 nm thick POEGMA brush coatings are capable of determining the response of cells, irrespective to the underlying

topology. Thus, polymer brushes decouple substrate micro-/nano-topology and the adhesion of stem cells. Brush film compliance, chain flexibility and controlled ligand exposure simultaneously act to determine the interfacial phenomena between biological medium and the biomaterial. These results emphasize the role of thin brushes as ECM-cell mediating layers, to decouple cells-topology interactions and to effectively mask any contact guidance or roughness effect. Due to their intrinsic robustness, high density and tunable configuration, polymer brushes have been demonstrated as effective components for the design of next-generation artificial ECM for homogenous stem cell preparations.

Associated Content

Supporting Information

Acknowledgements

This work was financially supported by the MESA+ Institute for Nanotechnology of the University of Twente and by the Technology foundation STW (STW, 11135). The authors thank Dr. M.A. Hempenius for the many useful discussions.

References

(1) Daley, W. P.; Peters, S. B.; Larsen, M., Extracellular matrix dynamics in development and regenerative medicine. *Journal of Cell Science* **2008,** *121,* 255-264.

(2) Guilak, F.; Cohen, D. M.; Estes, B. T.; Gimble, J. M.; Liedtke, W.; Chen, C. S., Control of Stem Cell Fate by Physical Interactions with the Extracellular Matrix. *Cell Stem Cell* **2009,** *5,* 17-26.

(3) Chamberlain, G.; Fox, J.; Ashton, B.; Middleton, J., Concise review: Mesenchymal stem cells: Their phenotype, differentiation capacity, immunological features, and potential for homing. *Stem Cells* **2007,** *25,* 2739-2749.

(4) Bianco, P.; Robey, P. G.; Simmons, P. J., Mesenchymal stem cells: Revisiting history, concepts, and assays. *Cell Stem Cell* **2008,** *2,* 313-319.

(5) Yim, E. K. F.; Pang, S. W.; Leong, K. W., Synthetic nanostructures inducing differentiation of human mesenchymal stem cells into neuronal lineage. *Exp. Cell Res.* **2007,** *313,* 1820-1829.

(6) Pittenger, M. F.; Mackay, A. M.; Beck, S. C.; Jaiswal, R. K.; Douglas, R.; Mosca, J. D.; Moorman, M. A.; Simonetti, D. W.; Craig, S.; Marshak, D. R., Multilineage Potential of Adult Human Mesenchymal Stem Cells. *Science* **1999,** *284,* 143-147.

(7) McBeath, R.; Pirone, D. M.; Nelson, C. M.; Bhadriraju, K.; Chen, C. S., Cell Shape, Cytoskeletal Tension, and RhoA Regulate Stem Cell Lineage Commitment. *Developmental Cell* **2004,** *6,* 483-495.

(8) Engler, A. J.; Sen, S.; Sweeney, H. L.; Discher, D. E., Matrix Elasticity Directs Stem Cell Lineage Specification. *Cell* **2006,** *126,* 677-689.

(9) Dalby, M. J.; Gadegaard, N.; Tare, R.; Andar, A.; Riehle, M. O.; Herzyk, P.; Wilkinson, C. D. W.; Oreffo, R. O. C., The control of human mesenchymal cell differentiation using nanoscale symmetry and disorder. *Nat. Mater.* **2007,** *6,* 997-1003.

(10) McMurray, R. J.; Gadegaard, N.; Tsimbouri, P. M.; Burgess, K. V.; McNamara, L. E.; Tare, R.; Murawski, K.; Kingham, E.; Oreffo, R. O. C.; Dalby, M. J., Nanoscale surfaces for the long-term maintenance of mesenchymal stem cell phenotype and multipotency. *Nat. Mater.* **2011,** *10,* 637-644.

(11) Trappmann, B.; Gautrot, J. E.; Connelly, J. T.; Strange, D. G. T.; Li, Y.; Oyen, M. L.; Stuart, M. A. C.; Boehm, H.; Li, B.; Vogel, V.; Spatz, J. P.; Watt, F. M.; Huck, W. T. S., Extracellular-matrix tethering regulates stem-cell fate. *Nat. Mater.* **2012,** *11,* 642-649.

(12) Shih, Y.-R. V.; Tseng, K.-F.; Lai, H.-Y.; Lin, C.-H.; Lee, O. K., Matrix Stiffness Regulation of Integrin-Mediated Mechanotransduction During Osteogenic Differentiation of Human Mesenchymal Stem Cells. *Journal of Bone and Mineral Research* **2011,** *26,* 730-738.

(13) Gittens, R. A.; McLachlan, T.; Olivares-Navarrete, R.; Cai, Y.; Berner, S.; Tannenbaum, R.; Schwartz, Z.; Sandhage, K. H.; Boyan, B. D., The effects of combined micron-/submicron-scale surface roughness and nanoscale features on cell proliferation and differentiation. *Biomaterials* **2011,** *32,* 3395-3403.

(14) Nandakumar, A.; Birgani, Z. T.; Santos, D.; Mentink, A.; Auffermann, N.; van der Werf, K.; Bennink, M.; Moroni, L.; van Blitterswijk, C.; Habibovic, P., Surface modification of electrospun fibre meshes by oxygen plasma for bone regeneration. *Biofabrication* **2013,** *5*.

(15) Unadkat, H. V.; Hulsman, M.; Cornelissen, K.; Papenburg, B. J.; Truckenmüller, R. K.; Carpenter, A. E.; Wessling, M.; Post, G. F.; Uetz, M.; Reinders, M. J. T.; Stamatialis, D.; van Blitterswijk, C. A.; de Boer, J., An algorithm-based topographical biomaterials library to instruct cell fate. *Proceedings of the National Academy of Sciences* **2011,** *108,* 16565-16570.

(16) Biggs, M. J. P.; Richards, R. G.; McFarlane, S.; Wilkinson, C. D. W.; Oreffo, R. O. C.; Dalby, M. J., Adhesion formation of primary human osteoblasts and the functional response of mesenchymal stem cells to 330 nm deep microgrooves. *J. R. Soc. Interface* **2008,** *5,* 1231-1242.

(17) Dalby, M. J.; Riehle, M. O.; Johnstone, H.; Affrossman, S.; Curtis, A. S. G., In vitro reaction of endothelial cells to polymer demixed nanotopography. *Biomaterials* **2002,** *23,* 2945-2954.

(18) Song, W.; Lu, H. X.; Kawazoe, N.; Chen, G. P., Adipogenic Differentiation of Individual Mesenchymal Stem Cell on Different Geometric Micropatterns. *Langmuir* **2011,** *27,* 6155-6162.

(19) Kilian, K. A.; Bugarija, B.; Lahn, B. T.; Mrksich, M., Geometric cues for directing the differentiation of mesenchymal stem cells. *Proceedings of the National Academy of Sciences* **2010,** *107,* 4872-4877.

(20) Ayres, N., Polymer brushes: Applications in biomaterials and nanotechnology. *Polymer Chemistry* **2010,** *1,* 769-777.

(21) Barbey, R.; Lavanant, L.; Paripovic, D.; Schuwer, N.; Sugnaux, C.; Tugulu, S.; Klok, H. A., Polymer Brushes via Surface-Initiated Controlled Radical Polymerization: Synthesis, Characterization, Properties, and Applications. *Chem. Rev.* **2009,** *109,* 5437-5527.

(22) Cooperstein, M. A.; Canavan, H. E., Biological Cell Detachment from Poly(N-isopropyl acrylamide) and Its Applications. *Langmuir* **2010,** *26,* 7695-7707.

(23) Hu, Z. B.; Cai, T.; Chi, C. L., Thermoresponsive oligo(ethylene glycol)-methacrylate-based polymers and microgels. *Soft Matter* **2010,** *6,* 2115-2123.

(24) Klein Gunnewiek, M.; Di Luca, A.; Sui, X.; van Blitterswijk, C. A.; Moroni, L.; Vancso, G. J., Controlled Surface Initiated Polymerization of N-Isopropylacrylamide from Polycaprolactone Substrates for Regulating Cell Attachment and Detachment. *Israel Journal of Chemistry* **2012,** *52,* 339-346.

(25) Navarro, M.; Benetti, E. M.; Zapotoczny, S.; Planell, J. A.; Vancso, G. J., Buried, Covalently Attached RGD Peptide Motifs in Poly(methacrylic acid) Brush Layers: The Effect of Brush Structure on Cell Adhesion. *Langmuir* **2008,** *24,* 10996-11002.

(26) Tugulu, S.; Silacci, P.; Stergiopulos, N.; Klok, H.-A., RGD--Functionalized polymer brushes as substrates for the integrin specific adhesion of human umbilical vein endothelial cells. *Biomaterials* **2007,** *28,* 2536-2546.

(27) Xu, F. J.; Wang, Z. H.; Yang, W. T., Surface functionalization of polycaprolactone films via surface-initiated atom transfer radical polymerization for covalently coupling cell-adhesive biomolecules. *Biomaterials* **2010,** *31,* 3139-3147.

(28) Xu, F. J.; Zheng, Y. Q.; Zhen, W. J.; Yang, W. T., Thermoresponsive poly(N-isopropyl acrylamide)-grafted polycaprolactone films with surface immobilization of collagen. *Colloid Surf. B-Biointerfaces* **2011,** *85,* 40-47.

(29) Konradi, R.; Acikgoz, C.; Textor, M., Polyoxazolines for Nonfouling Surface Coatings — A Direct Comparison to the Gold Standard PEG. *Macromolecular Rapid Communications* **2012,** *33,* 1663-1676.

(30) Jiang, S.; Cao, Z., Ultralow-Fouling, Functionalizable, and Hydrolyzable Zwitterionic Materials and Their Derivatives for Biological Applications. *Advanced Materials* **2010,** *22,* 920-932.

(31) Liu, Q. S.; Singh, A.; Lalani, R.; Liu, L. Y., Ultralow Fouling Polyacrylamide on Gold Surfaces via Surface-Initiated Atom Transfer Radical Polymerization. *Biomacromolecules* **2012,** *13,* 1086-1092.

(32) Raynor, J. E.; Petrie, T. A.; García, A. J.; Collard, D. M., Controlling Cell Adhesion to Titanium: Functionalization of Poly[oligo(ethylene glycol)methacrylate] Brushes with Cell-Adhesive Peptides. *Advanced Materials* **2007,** *19,* 1724-1728.

(33) Xu, F. J.; Liu, L. Y.; Yang, W. T.; Kang, E. T.; Neoh, K. G., Active Protein-Functionalized Poly(poly(ethylene glycol) monomethacrylate)-Si(100) Hybrids from Surface-

Initiated Atom Transfer Radical Polymerization for Potential Biological Applications. *Biomacromolecules* **2009,** *10,* 1665-1674.

(34) Tugulu, S.; Klok, H.-A., Surface Modification of Polydimethylsiloxane Substrates with Nonfouling Poly(Poly(ethylene glycol)methacrylate) Brushes. *Macromolecular Symposia* **2009,** *279,* 103-109.

(35) Edmondson, S.; Osborne, V. L.; Huck, W. T. S., Polymer brushes via surface-initiated polymerizations. *Chemical Society Reviews* **2004,** *33,* 14-22.

(36) Ma, H.; Hyun, J.; Stiller, P.; Chilkoti, A., "Non-Fouling" Oligo(ethylene glycol)-Functionalized Polymer Brushes Synthesized by Surface-Initiated Atom Transfer Radical Polymerization. *Advanced Materials* **2004,** *16,* 338-341.

(37) Brown, A. A.; Khan, N. S.; Steinbock, L.; Huck, W. T. S., Synthesis of oligo(ethylene glycol) methacrylate polymer brushes. *European Polymer Journal* **2005,** *41,* 1757-1765.

(38) Le, D. M.; Kulangara, K.; Adler, A. F.; Leong, K. W.; Ashby, V. S., Dynamic Topographical Control of Mesenchymal Stem Cells by Culture on Responsive Poly(epsilon-caprolactone) Surfaces. *Advanced Materials* **2011,** *23,* 3278-+.

(39) Lendlein, A.; Schmidt, A. M.; Schroeter, M.; Langer, R., Shape-memory polymer networks from oligo(epsilon-caprolactone)dimethacrylates. *J. Polym. Sci. Pol. Chem.* **2005,** *43,* 1369-1381.

(40) Ping, P.; Wang, W. S.; Chen, X. S.; Jing, X. B., Poly(epsilon-caprolactone) polyurethane and its shape-memory property. *Biomacromolecules* **2005,** *6,* 587-592.

(41) Woodruff, M. A.; Hutmacher, D. W., The return of a forgotten polymer--Polycaprolactone in the 21st century. *Progress in Polymer Science* **2010,** *35,* 1217-1256.

(42) Andersson, A. S.; Backhed, F.; von Euler, A.; Richter-Dahlfors, A.; Sutherland, D.; Kasemo, B., Nanoscale features influence epithelial cell morphology and cytokine production. *Biomaterials* **2003,** *24,* 3427-3436.

(43) Guvendiren, M.; Burdick, J. A., The control of stem cell morphology and differentiation by hydrogel surface wrinkles. *Biomaterials* **2010,** *31,* 6511-6518.

(44) Watari, S.; Hayashi, K.; Wood, J. A.; Russell, P.; Nealey, P. F.; Murphy, C. J.; Genetos, D. C., Modulation of osteogenic differentiation in hMSCs cells by submicron topographically-patterned ridges and grooves. *Biomaterials* **2012,** *33,* 128-136.

(45) Kulangara, K.; Yang, Y.; Yang, J.; Leong, K. W., Nanotopography as modulator of human mesenchymal stem cell function. *Biomaterials* **2012,** *33,* 4998-5003.

(46) Ponsonnet, L.; Reybier, K.; Jaffrezic, N.; Comte, V.; Lagneau, C.; Lissac, M.; Martelet, C., Relationship between surface properties (roughness, wettability) of titanium and titanium alloys and cell behaviour. *Materials Science and Engineering: C* **2003,** *23,* 551-560.

(47) Samaroo, H. D.; Lu, J.; Webster, T. J., Enhanced endothelial cell density on NiTi surfaces with sub-macron to nanometer roughness. *Int. J. Nanomed.* **2008,** *3,* 75-82.

(48) Massia, S. P.; Hubbell, J. A., An RGD spacing of 440 nm is sufficient for integrin alpha V beta 3-mediated fibroblast spreading and 140 nm for focal contact and stress fiber formation. *The Journal of Cell Biology* **1991,** *114,* 1089-1100.

(49) Cook, A. D.; Hrkach, J. S.; Gao, N. N.; Johnson, I. M.; Pajvani, U. B.; Cannizzaro, S. M.; Langer, R., Characterization and development of RGD-peptide-modified poly(lactic acid-co-lysine) as an interactive, resorbable biomaterial. *Journal of Biomedical Materials Research* **1997,** *35,* 513-523.

(50) Webb, K.; Hlady, V.; Tresco, P. A., Relationships among cell attachment, spreading, cytoskeletal organization, and migration rate for anchorage-dependent cells on model surfaces. *Journal of Biomedical Materials Research* **2000,** *49,* 362-368.

(51) Keselowsky, B. G.; Collard, D. M.; Garcia, A. J., Surface chemistry modulates fibronectin conformation and directs integrin binding and specificity to control cell adhesion. *Journal of Biomedical Materials Research Part A* **2003,** *66A,* 247-259.

(52) Dolatshahi-Pirouz, A.; Jensen, T. H. L.; Kolind, K.; Bünger, C.; Kassem, M.; Foss, M.; Besenbacher, F., Cell shape and spreading of stromal (mesenchymal) stem cells cultured on fibronectin coated gold and hydroxyapatite surfaces. *Colloids and Surfaces B: Biointerfaces* **2011,** *84,* 18-25.

(53) Discher, D. E.; Janmey, P.; Wang, Y. L., Tissue cells feel and respond to the stiffness of their substrate. *Science* **2005,** *310,* 1139-1143.

(54) Nam, K.; Fukaya, R.; Hashimoto, Y.; Ito, Y.; Kimura, T.; Kishida, A., Human Mesenchymal Stem Cell Behavior on Concentrated Polymer Brushes Presenting Different Surface Stiffness. *Chemistry Letters* **2010,** *39,* 1164-1165.

(55) Loesberg, W. A.; te Riet, J.; van Delft, F. C. M. J. M.; Schön, P.; Figdor, C. G.; Speller, S.; van Loon, J. J. W. A.; Walboomers, X. F.; Jansen, J. A., The threshold at which substrate nanogroove dimensions may influence fibroblast alignment and adhesion. *Biomaterials* **2007,** *28,* 3944-3951.

(56) van Delft, F. C. M. J. M.; van den Heuvel, F. C.; Loesberg, W. A.; te Riet, J.; Schön, P.; Figdor, C. G.; Speller, S.; van Loon, J. J. W. A.; Walboomers, X. F.; Jansen, J. A., Manufacturing substrate nano-grooves for studying cell alignment and adhesion. *Microelectronic Engineering* **2008,** *85,* 1362-1366.

(57) Wieringa, P.; Tonazzini, I.; Micera, S.; Cecchini, M., Nanotopography induced contact guidance of the F11 cell line during neuronal differentiation: a neuronal model cell line for tissue scaffold development. *Nanotechnology* **2012,** *23,* 275102-275102.

(58) Balloni, S.; Calvi, E. M.; Damiani, F.; Bistoni, G.; Calvitti, M.; Locci, P.; Becchetti, E.; Marinucci, L., Effects of Titanium Surface Roughness on Mesenchymal Stem Cell Commitment and Differentiation Signaling. *Int. J. Oral Maxillofac. Implants* **2009,** *24,* 627-635.

(59) Hu, X.; Park, S.-H.; Gil, E. S.; Xia, X.-X.; Weiss, A. S.; Kaplan, D. L., The influence of elasticity and surface roughness on myogenic and osteogenic-differentiation of cells on silk-elastin biomaterials. *Biomaterials* **2011,** *32,* 8979-8989.

(60) Yu, B.-Y.; Chen, P.-Y.; Sun, Y.-M.; Lee, Y.-T.; Young, T.-H., Response of Human Mesenchymal Stem Cells (hMSCs) to the Topographic Variation of Poly(3-Hydroxybutyrate-co-3-Hydroxyhexanoate) (PHBHHx) Films. *Journal of Biomaterials Science-Polymer Edition* **2012,** *23,* 1-26.

Keyword: cell morphology; mesenchymal stem cells; poly(ε-caprolactone); polymer brushes; surface topology

Michel Klein Gunnewiek, Edmondo M. Benetti, Andrea Di Luca, Clemens A. van Blitterswijk, Lorenzo Moroni, and G. Julius Vancso**

Thin Polymer Brush Decouples Biomaterial's Micro-/Nano-topology and Stem Cell Adhesion

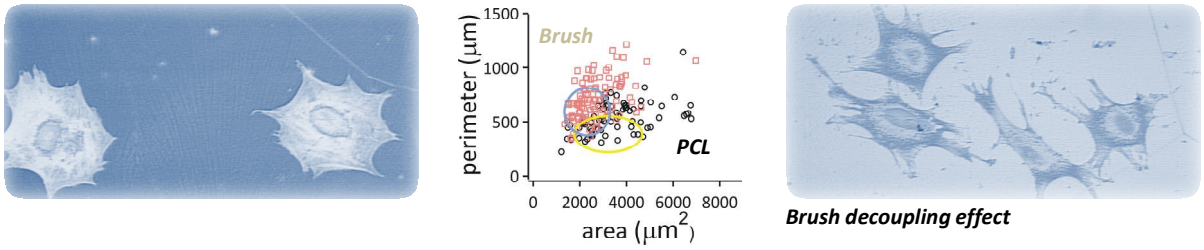

POEGMA polymer brushes are proven to decouple the interaction between a rough surface and adhering human Mesenchymal Stem Cells (hMSCs). On PCL surfaces, hMSCs are spreading and elongating differently depending on the PCL feature (spherulite) size. After growing POEGMA polymer brushes from the surface, the cells are behaving uniformly, independent on the underlying surface structure.